Separation Science and Technology
Publication details, including instructions for authors and subscription information:
http://www.informaworld.com/smpp/title~content=t713708471

Separation of Carbon Black from Silica by Froth Flotation Part 1: Effect of Operational Parameters

Pisan Chungchamroenkit[a]; Sumaeth Chavadej[a]; John F. Scamehorn[b]; Ummarawadee Yanatatsaneejit[a]; Boonyarach Kitiyanan[a]
[a] The Petroleum and Petrochemical College, Chulalongkorn University, Bangkok, Thailand [b] Institute for Applied Surfactant Research, University of Oklahoma, Norman, OK, USA

To cite this Article Chungchamroenkit, Pisan , Chavadej, Sumaeth , Scamehorn, John F. , Yanatatsaneejit, Ummarawadee and Kitiyanan, Boonyarach(2009) 'Separation of Carbon Black from Silica by Froth Flotation Part 1: Effect of Operational Parameters', Separation Science and Technology, 44: 1, 203 — 226

To link to this Article: DOI: 10.1080/01496390802281968

URL: http://dx.doi.org/10.1080/01496390802281968

Separation Science and Technology, 44: 203–226, 2009
Copyright © Taylor & Francis Group, LLC
ISSN: 0149-6395 print/1520-5754 online
DOI: 10.1080/01496390802281968

Separation of Carbon Black from Silica by Froth Flotation Part 1: Effect of Operational Parameters

Pisan Chungchamroenkit,[1] Sumaeth Chavadej,[1] John F. Scamehorn,[2] Ummarawadee Yanatatsaneejit,[1] and Boonyarach Kitiyanan[1]
[1]The Petroleum and Petrochemical College, Chulalongkorn University, Bangkok, Thailand
[2]Institute for Applied Surfactant Research, University of Oklahoma, Norman, OK, USA

Abstract: Froth flotation can be applied to separate hydrophobic particles from hydrophilic ones in aqueous solution with the use of an appropriate surfactant. In this work, carbon black was separated from silica gel by means of froth flotation. Since the point of zero charge, or PZC, of the carbon black (3.5) is close to that of the silica gel (4.1), a nonionic surfactant (ethoxylated alcohol) was selected as the separating agent. Based on experimental results using a surfactant concentration of 62 μM or 75% of its critical micelle concentration (CMC), up to 70% of carbon black recovery was achieved with a carbon black enrichment ratio around 3.5. Added electrolyte (NaCl) showed a negligible effect on the separation efficiency. The presence of the surfactant was found to provide both a higher mass transfer surface area and to reduce the coalescence of air bubbles in the froth flotation column.

Keywords: Carbon black, froth flotation, nonionic surfactant

Received 27 February 2008; accepted 4 June 2008.

Address correspondence to Sumaeth Chavadej, Chulalongkorn University, The Petroleum and Petrochemical College, Chula Soi 12, Phythai Road, Bangkok 10330, Thailand. E-mail: sumaeth.c@chula.ac.th

INTRODUCTION

Froth flotation is a surfactant-based separation process (1) which is widely used in various applications such as mineral processing (2) and paper deinking (3). There are several advantages of flotation, such as its rapid operation, minimal space requirements, high removal efficiency, and low operational costs (4). In a typical froth flotation operation, air is sparged into the surfactant solution at the bottom of the column through a sintered glass disk. With the aid of a surfactant, hydrophobic particles such as carbon black attach to the air bubbles and are carried to the top of the column (5) where these particles accumulate in the froth, which can be skimmed off. To obtain a highly selective separation in froth flotation, an appropriate surfactant is added to create the conditions where the silica gel particles do not tend to adhere to the air bubbles, while the carbon black is selectively carried over in the froth. The objective of this work was to demonstrate the relatively inexpensive method of froth flotation in separating hydrophobic from hydrophilic particles having similar surface charges, as indicated by the point of zero charge (PZC).

Single-walled carbon nanotubes (SWNTs) (6,7) have illustrated their potential in many applications (8). The required purity of SWNTs varies with the application (9). Production of SWNTs via the supported catalyst is a method to produce SWNTs economically (10). However, residual catalysts and the catalyst support can contaminate the as-produced SWNTs. The silica catalyst support as an impurity in SWNTs is of particular concern. To purify these products, the bond between the SWNTs and the silica gel support must be broken, followed by a physical separation step to separate the silica gel particles from the SWNTs.

The froth flotation technique proposed here has the potential to achieve a selective separation between SWNTs and silica. Since carbon black and SWNTs both have hydrophobic surfaces, there may be analogies between the separation of the two substrates from silica. At least, this study of carbon black can help define the role of hydrophobicity versus other factors when comparing these results to carbon nanotube froth flotation in a later study. We do not want to overemphasize the analogy between carbon black and carbon nanotubes due to the substantial difference in particle size and the van der Waals interactions between carbon nanotubes that causes them to bundle (11). Future work will involve the purification of as-produced SWNTs by froth flotation.

EXPERIMENTAL

Materials

Carbon black, type 400 R, having an average particle size of 0.24 μm and a bulk density of 0.3 g/cm^3, was supplied by Cabot Company, USA. The as-received carbon black was rinsed with deionized water, centrifuged, and dried overnight at 120°C to remove all impurities before use. Silica gel having an average particle size of 62–210 μm (70–230 mesh), an average pore diameter of 6 nm, and a density of 1.5 g/cm^3, was supplied by Aldrich Chemical Company, USA. Surfonic L24–7, a nonionic surfactant with a high purity of 100%, composed of linear alcohol polyethoxylate, with an average degree of polymerization of 7 and a linear alkyl chain of 12–14 carbon number, was obtained from Huntsman Company, USA, and used as received. Hydrochloric acid with a concentration of 37%, sodium hydroxide with a purity of 99%, and sodium chloride with a purity of 99% were obtained from Labscan Asia Company, Thailand. Deionized water was used to prepare all solutions throughout this work.

Methodology

Measurement of Point of Zero Charge (PZC) and Contact Angle

To measure the PZC of either carbon black or silica gel, 10 mL of aqueous solutions having different pH values ranging from 1 to 11 were prepared in vials by adding hydrochloric acid or sodium hydroxide to deionized water with an initial pH of 6.2. The ionic strength of the solutions was kept constant at 0.1 M by using sodium chloride to more quickly attain a state of equilibrium without affecting the final pH (12). After that, 0.5 g of carbon black or silica gel was added to each vial, stirred and then left overnight to equilibrate at 25 ± 1°C. The equilibrium pH was then measured and plotted against the initial pH for each substrate. The PZC can be readily obtained from the point at which the initial pH equals the equilibrium pH.

The contact angle of the solid was determined by grinding and then pressing the powder of the carbon black or the silica gel with a hydraulic press under a pressure of 15 N/m^2 to obtain flat surface pellets. The pellets were then used to measure the contact angle by a drop shape analysis system (Krüss, DSA10-Mk2) with the sessile drop method using a drop of 5 μL of deionized water or surfactant solutions at room temperature (26 ± 1°C).

Surfactant Adsorption Experiment and CMC Determination

The surfactant adsorption onto carbon black and silica gel was studied at 25 ± 1°C. Carbon black or silica gel (0.1 g) was mixed with 20 mL of a surfactant solution having different initial concentrations. The mixture was well shaken and allowed to equilibrate for three days, which has been shown to be sufficient for equilibrium to be attained. After that, it was centrifuged at 15,000 rpm for 30 min. The supernatant was decanted and the equilibrium surfactant concentration in the supernatant was analyzed by a total organic carbon analyzer (Shimadzu, TOC – V_{CSH}). The specific surface areas of both the carbon black and the silica gel were measured by using a surface area analyzer (Sorptomatic, Thermo Finnigan, 1990).

To measure the critical micelle concentration (CMC) of the surfactant, the surface tensions of aqueous solutions containing various surfactant concentrations were measured at room temperature by using a DuNouy-Ring tensiometer (Krüss, K10ST). The CMC of surfactant was determined from the concentration at which the surface tension reaches a plateau (13).

Froth Flotation Experiments

A schematic of the froth flotation apparatus used in this work is shown in Fig. 1. The flotation column was a glass tube with an inside diameter of 3.8 cm and a length of 120 cm. In this study, the composition of the solid mixture was fixed at 25 wt.% carbon black and 75 wt.% silica gel. A surfactant solution of 750 mL, having different surfactant concentrations,

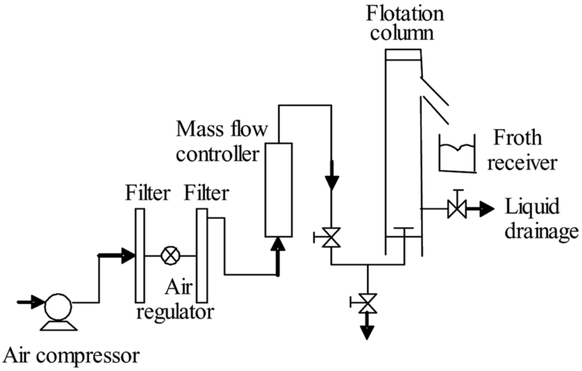

Figure 1. Schematic of the froth flotation apparatus.

and the solid mixture sample, having different total weights, were well mixed. The resultant mixture solution was then transferred to the flotation column. Air was introduced at the bottom of the column through a sintered glass disk having pore size diameters of about 16–40 μm. The air flow rate was varied from 150 to 300 mL/min by using a mass flow controller (AALBORG, GFC171S). The initial surfactant concentration was varied in the range of 0.25–1 times the CMC.

During the froth flotation experiments, the generated foam was collected at the top of the column until no further foam was generating out of the column due to surfactant depletion. Typical run times were 15 to 20 minutes. Then, the collected foam was allowed to collapse to analyze the total dried weights of carbon black and silica gel in the overhead froth. All of the flotation experiments were performed at room temperature. To get rid of the remaining surfactant, deionized water was added to the foamate (collapsed foam), followed by centrifugation to obtain the solid residue. This step was repeated a few times. After that, the solid was dried in an oven at 110°C to obtain the total dried weight. The purity of carbon black in the dried solid samples was determined by mass balance after the carbon black fraction was completely oxidized in air at 700°C and the sample reweighed.

Foam Characteristics

Foam characteristic experiments were also conducted independently in the same flotation column. After a mixture solution, having different concentrations of solid mixture and surfactant, was transferred to the column and well mixed, filtered air was introduced at the bottom of the column at a desired flow rate until a maximum foam height was achieved. The maximum foam height divided by the initial solution height in the column is defined as foamability. The introduction of air to the column was then stopped and the time required for the foam volume to collapse to one half of the maximum height was used to quantify foam stability ($t_{1/2}$).

Air Bubble Size Measurements

The measurement of air bubble sizes was conducted in the same column that was used in the froth flotation experiments. The images of the air bubbles in the flotation column were taken at different times and different positions in the column by using a color video camera (Sony, SSC-DC58AP). In order to minimize the curvature effect on the images taken by the camera, two points on the centerline of the column were used for taking the photographs: one-third (position 1) and two-thirds (position 2) of the initial liquid height based on the solution bottom. For each point, 100 photographs were taken every 5 min, and the total lag time, due to the image recording process and the camera moving from position 1 to position 2, was less than 30 s. For each photograph, at least 500 air bubbles were fitted to evaluate the diameters of individual bubbles and then the average bubble diameter and the bubble size distribution were calculated by using the Image-Pro Plus software.

RESULTS AND DISCUSSION

Point of Zero Charge (PZC) and Contact Angle

The equilibrium pH as a function of initial pH for carbon black and silica gel is shown in Fig. 2. The crossing point of each curve with the y = x line corresponds to the PZC of the solid sample. From the figure, the PZC values of carbon black and silica gel are 3.5 and 4.1, respectively. Therefore, the surfaces of both solids become negatively charged when exposed to a solution pH above 4.1 and positively charged at a pH lower than 3.5. Moreover, as shown in Fig. 3, the solution pH decreases with increasing weight of solid particles (with an initial pH of 6.2). Interestingly, the effect of the weight of carbon black was obviously more significant than

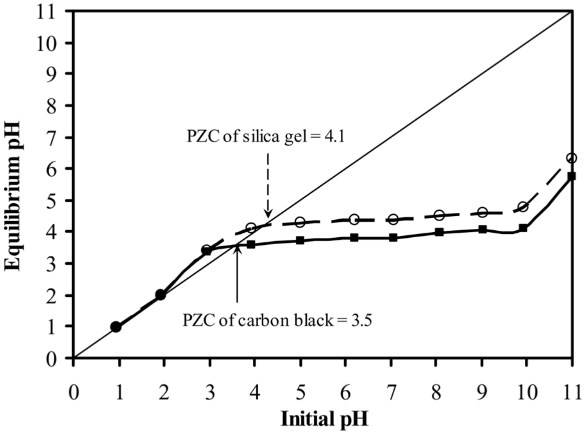

Figure 2. Determination of point of zero charge (PZC) for carbon black and silica gel at a solid loading of 50 g/L.

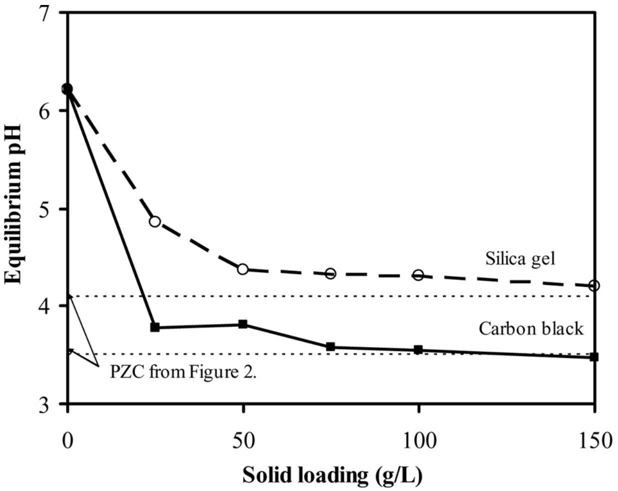

Figure 3. pH changes upon the addition of carbon black or silica gel into water with an initial pH of 6.2.

that of silica gel. The pH of the solution changes from the initial pH toward the PZC. The final pH approaches the PZC at a high enough solid loading. The final pH values of these two solids, as shown in Fig. 3 at high solid loadings, are consistent with the PZC values deduced from Fig. 2. An ionic surfactant may not provide good selective separation of carbon black from silica gel because the PZC values of carbon black and silica gel are not significantly different. Consequently, a nonionic surfactant was selected for use in this study.

In the froth flotation process, particles are selectively separated based on several factors, including the differences in surface wettability. The addition of surfactant into water reduces the liquid-vapor surface tension as well as the liquid-solid interfacial tension, which increases the wettability on the particle surfaces or reduces the contact angle of liquid on the solid. As shown in Fig. 4, carbon black has an average contact angle with deionized water of 59.8°, whereas silica gel has an average contact angle with deionized water of 15.8°. From Fig. 4, as the surfactant concentration increases about the CMC, the contact angles of both carbon black and silica gel reach their minimum values. The difference between the contact angles of the carbon black and the silica is smaller as the surfactant solution concentration increases up to the CMC, and the difference is unchanged in the range of 1.0 to 2.5 times the CMC. Even above

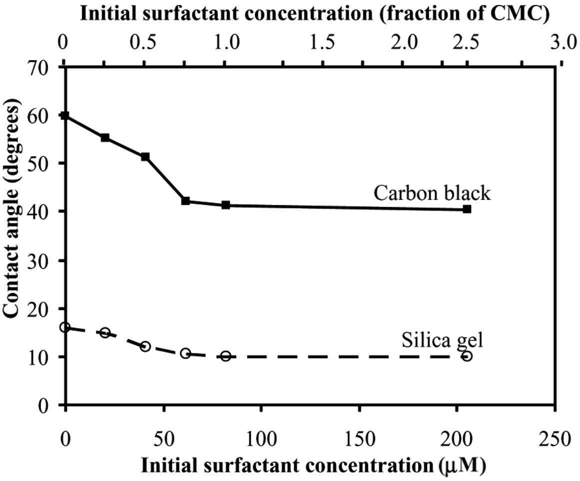

Figure 4. Contact angle of carbon black and silica gel as a function of initial surfactant concentration.

the CMC, the difference in contact angles between carbon and silica is about 30°.

Surfactant Adsorption Isotherms and CMC

The CMC of the studied surfactant is 82.1 μM, in agreement with literature CMC values for this type of surfactant structure (14). The adsorption isotherms of surfactant on carbon black and silica gel are depicted in Fig. 5. The specific surface areas of carbon black and silica gel are 132.5 and 403.7 m^2/g, respectively. The amount of adsorbed surfactant is then reported on the basis of unit surface area. As expected, the surfactant adsorption reaches a plateau at about the CMC. The reason the surfactant adsorption levels off above the CMC is that the chemical potential of the surfactant in solution becomes constant there, not because the surface of the solid is saturated (15). In the froth flotation operation, the surfactant present in the system can adsorb on all surfaces including carbon black, silica gel, and air bubbles. The amount of surfactant adsorbed at the air/water water interface is generally negligible when compared to the total amount of surfactant. Moreover, under the studied conditions, based on the maximum adsorption of surfactant on solid/liquid interfaces, the majority of the surfactant (more than 90%) will remain in the bulk

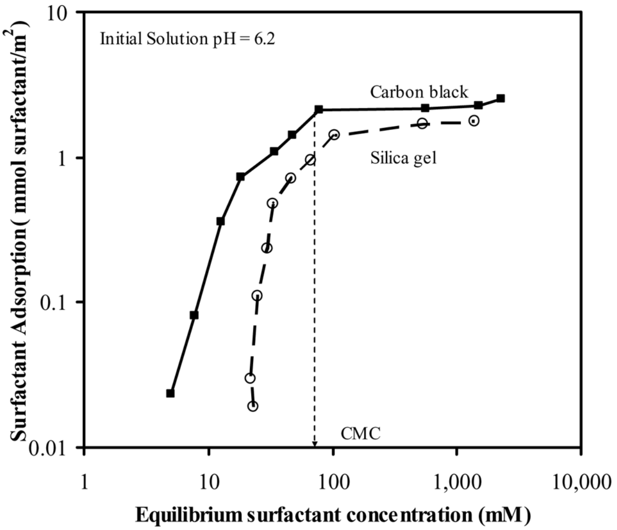

Figure 5. Adsorption isotherm of surfactant on carbon black and silica gel.

solution. Therefore, the bulk concentration of the surfactant is approximately equal to the initial surfactant concentration.

Froth Flotation Performance Results

The separation efficiency of the froth flotation column is quantified by both the recovery and the enrichment ratio of carbon black. The recovery of carbon black is defined as the weight of carbon black in the foamate as a percentage of the weight of the carbon black in the initial feed. The enrichment ratio of carbon black is the ratio of fraction of carbon black in the total solid recovered from the foamate to the fraction of carbon black in the total solid that is in the initial feed. An enrichment ratio greater than one indicates the selective separation of carbon black. The total surfactant loss can affect process economics. It is defined as a total weight of surfactant adsorbing onto the total particles (carbon black and silica gel) in the foamate divided by the weight of recovered carbon black. The amount of surfactant adsorbing onto the carbon black and silica gel were calculated from the adsorption isotherms. However, even though the total surfactant loss was calculated from the equilibrium adsorption of the surfactant on the solid particles, but the particles were only present in the solution containing the surfactant for a few minutes.

Therefore, the equilibrium surfactant adsorption is not attained during the froth flotation operation. As a result, the total surfactant loss reported can be considered as the maximum loss.

Effect of Initial Surfactant Concentration

In a froth flotation operation, the presence of surfactant plays an important role in both promoting and stabilizing the foam (16). From the previous studies of froth flotation to remove emulsified oil from water (17–20), the separation efficiency was found to be highest at a surfactant concentration which corresponds to the maximum values of both foam formation (foamability) and foam stability. Figure 6 shows the effect of surfactant concentration on foam characteristics. As surfactant concentration increased, the foamability increased; whereas the foam stability decreased. Maximum foamability or foam formation was found to be around the CMC, which is generally observed in other surfactant systems (15). However, the relationship of foam stability to surfactant concentration is more complicated and system-dependent.

Figure 7 shows the recovery and the enrichment ratio of carbon black, and the total surfactant loss as a function of surfactant concentration. For the conditions studied here, the carbon black recovery as high

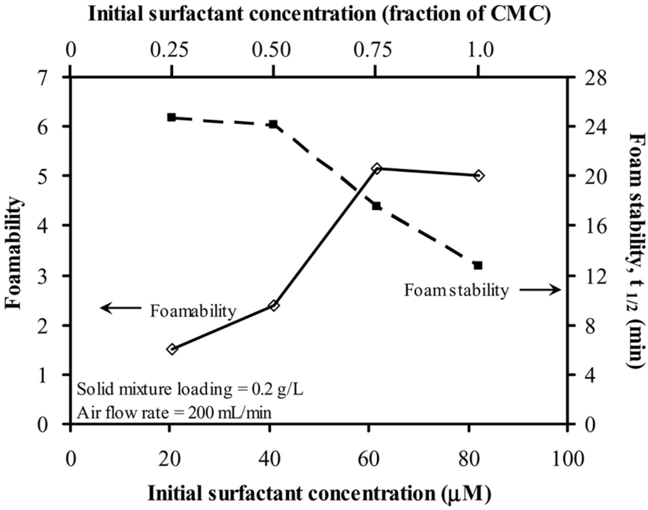

Figure 6. Effect of initial surfactant concentration on foamability and foam stability.

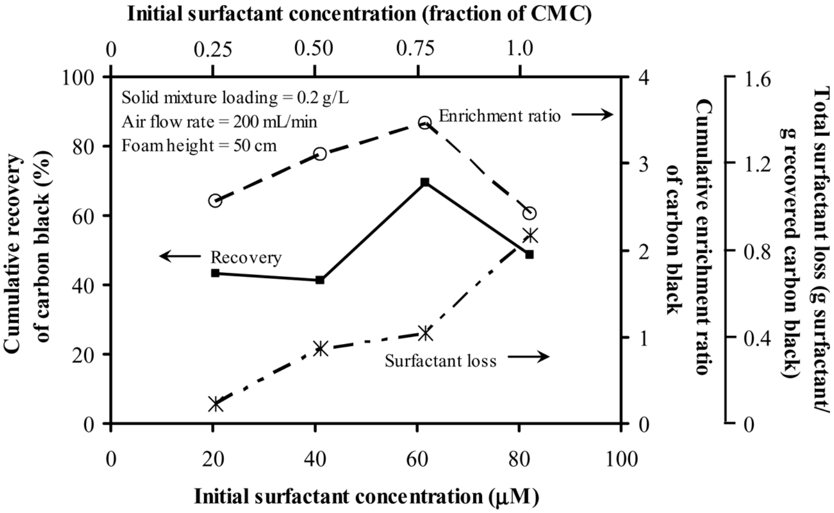

Figure 7. Effect of initial surfactant concentration on the recovery and enrichment ratio of carbon black and on surfactant loss.

as 70% and the enrichment ratio of carbon black as high as 3.5 demonstrate the technical feasibility of froth flotation for the selective separation of carbon black from silica gel. At surfactant concentrations in the range of 0.25 to 0.75 times the CMC, the carbon black recovery increased with increasing surfactant concentration. However, as observed in Fig. 7, when the surfactant concentration approaches the CMC, both the recovery and the enrichment ratio of carbon black decrease substantially. In addition, the monotonically increasing surfactant loss with increasing surfactant concentration obviously suggests that the surfactant loss is dependent on both the carbon black recovery and the adsorbed surfactant concentration as a function of the initial concentration. By comparing Figs. 6 and 7, both high foamability and high foam stability are needed to achieve a high carbon black recovery and a high carbon black enrichment ratio. The offsetting trends of increasing foamability and decreasing foam stability with increasing surfactant concentration result in an optimum surfactant concentration of around 0.75 times the CMC, so this initial surfactant concentration was used for further investigation in this work. Since the surfactant adsorption isotherms on carbon black and silica gel are similar (Fig. 5), and the interaction between particles and air bubbles and foam lamellae are complex, a fundamental interpretation of selectivity is difficult. From Fig. 4, the difference between the contact angles of the carbon black and silica gel increases with decreasing initial surfactant concentration, which may relate to increasing selectivity in the separation. However, the surfactant concentration should be high enough to generate foam to carry the carbon black particles to the column overhead. The trade-off between the contact angle and the foamability may be a factor that affects the carbon black selectivity. Moreover, since silica gel has a higher density than carbon black, the silica gel tends to settle faster due to gravity than the carbon black, augmenting the enrichment ratio of carbon black, which is always greater than one in this study; so carbon black is floated selectively compared to silica gel.

Effect of Solid Mixture Loading

Influence of the solid mixture loading in the feed solution on the foam characteristics and the separation efficiency are shown in Figs. 8 and 9, respectively. Up to 0.2 g/L solid loading, both foamability and foam stability remained constant, but at higher loadings, they declined dramatically with increasing solid loading. Hydrophobic particles, like carbon black, commonly act as antifoams or defoamers, while hydrophilic particles, like silica gel, can stabilize or destabilize foam (21); so a dramatic reduction in foamability and foam stability at high solid loadings is expected. The modest decrease in the recovery of carbon black with increased solid loading above 0.2 g/L is probably related to the decreases in both foamability and foam stability. Interestingly, in the solid loading range of 0.2–0.4 g/L, the enrichment ratio remained almost constant. Since the recovery is on a percentage basis, the total weight of carbon

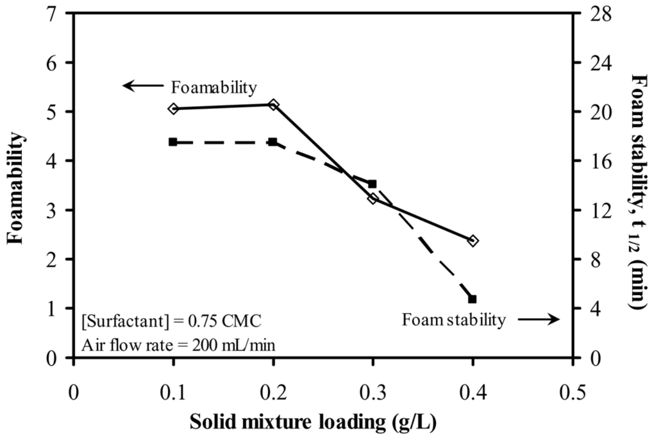

Figure 8. Effect of solid mixture loading on foamability and foam stability.

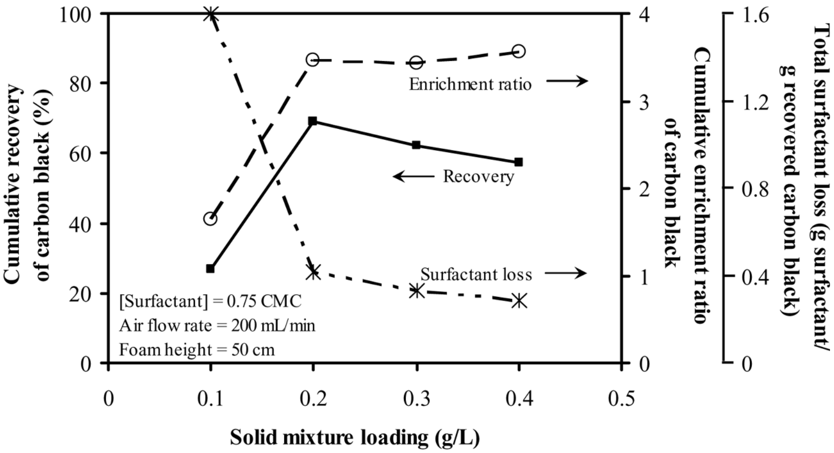

Figure 9. Effect of solid mixture loading on the recovery and enrichment ratio of carbon black and on surfactant loss.

black recovered actually increases as the solid loading increased above 0.2 g/L. Increased solid loading does not cause the carbon black recovery to decrease as significantly as would be expected from the dramatic decrease in foamability and foam stability, but in fact causes carbon black recovery to decrease drastically between solid loadings of 0.1 and 0.2 g/L. The reasons for these effects are unclear. A total surfactant loss (total unrecoverable surfactant per weight of recovered carbon black) from Fig. 9 is as low as 0.3 g surfactant/g recovered carbon black, which is equivalent to about 20 wt.% of the initial amount of surfactant. Since the highest carbon black recovery occurred at 0.2 g/L solid loading, this condition was used in subsequent experiments as a base condition.

Effect of Air Flow Rate

Both bubble size and volumetric flow rate of air influence the separation efficiency in froth flotation (22). The bubble size distribution will be discussed later. The effects of the air flow rate on the foam characteristics and on the separation efficiency of carbon black are shown in Figs. 10 and 11, respectively. The foamability was found to be nearly constant at an air flow rate below 250 mL/min, but it greatly increased at a flow rate above 250 mL/min. In contrast, the foam stability was almost invariant in the studied range of air flow rate. To obtain separation, a certain minimum air flow rate is required to cause any foam to flow from the top

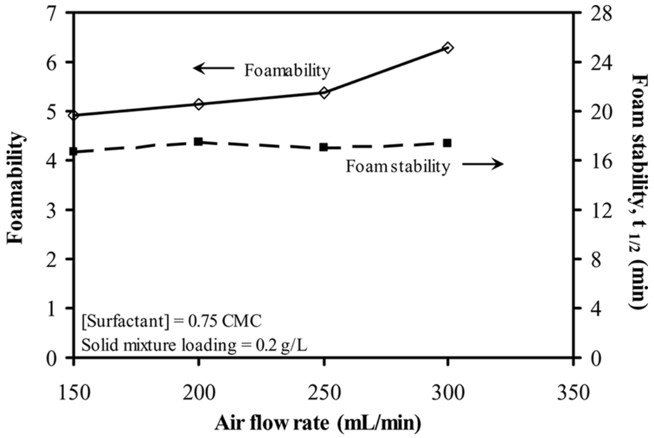

Figure 10. Effect of air flow rate on foamability and foam stability.

of the column. When air flow rate increases above this minimum required flowrate, 150 mL/min to 200 mL/min, carbon black recovery increases with increasing air flow rate, as observed in Fig. 11. However, if the air flow rates increased above 200 mL/min, the trend of the recovery of carbon black reverses. This may be due to the increased turbulence altering the flow pattern in the column to a severe circulation velocity in the solution, and some portion of carbon black attached to the bubble surface is carried back into the solution by this turbulence effect.

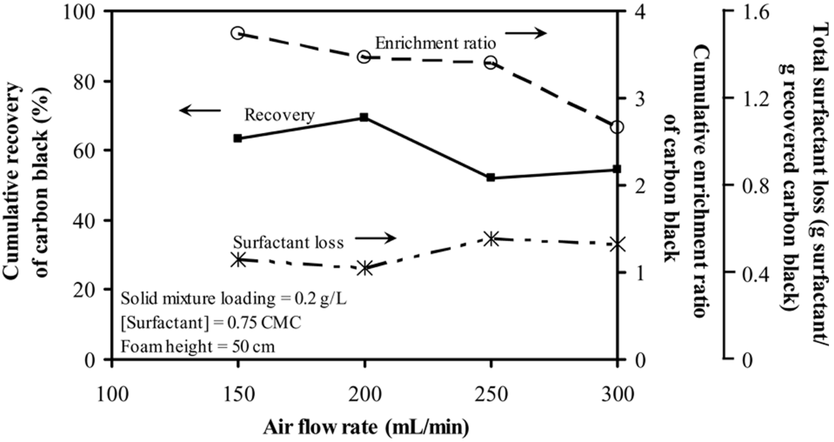

Figure 11. Effect of air flow rate on the recovery and enrichment ratio of carbon black and on surfactant loss.

Consequently, carbon black recovery is reduced at high air flow rates between 200 and 250 mL/min. However, at a much higher air flow rate (300 mL/min), the carbon black recovery was found to increase moderately as compared to that at 250 mL/min because the foamability at this point increased. This can be explained by the fact that at this very high air flow rate, the effect of foamability or foam production rate is more significant than that of foam stability. From Fig. 11, the enrichment ratio of carbon black monotonically decreased, but the total surfactant loss slightly increased with increasing air flow rate. This implies that carbon black selectively attaches to air bubbles rising through the solution and/or to the air/water interface in the foam lamellae. However, at very high air flow rates, the violent turbulence in the solution causes the physical attachment to be relatively less important than the gross flow effects causing flotation; overcoming the particle density differences which cause silica gel to preferentially settle, for example. Since the maximum observed carbon black recovery occurred at an air flow rate of 200 mL/min, this condition was selected as the base case for further experiments.

Effect of Initial Foam Height

A greater foam height results in a greater residence time, causing more foam drainage to occur before the foam overflows from the column; so foam height is one of the important operating parameters affecting the separation performance of a froth flotation unit. In this study, the froth flotation column was designed by fixing the height of the column, so the effect of initial foam height was investigated by changing the volume of the feed surfactant solution. The enrichment ratio and the recovery of carbon black and the total surfactant loss as a function of initial foam height are shown in Fig. 12. As initial foam height increases, the residence time of the particles in the foam lamellae increases, increasing settling time, reducing solid flow rate overheads, leading to the reduction of carbon black recovery with increasing foam height, as seen in Fig. 12, above a foam height of 50 cm. Also, due to foam drainage, foam flow rates also decrease with increasing foam height. However, at too low of a foam height, there is insufficient space for the foam to separate from the entrained liquid, so separation is poor, as seen by the low carbon black recovery, at a height of 30 cm. In addition, the enrichment ratio of carbon black increased only modestly, whereas the total surfactant loss significantly increased, with increasing foam height above 50 cm. Based on the results in Fig. 12, a foam height of 50 cm was selected as the base case for further experiments.

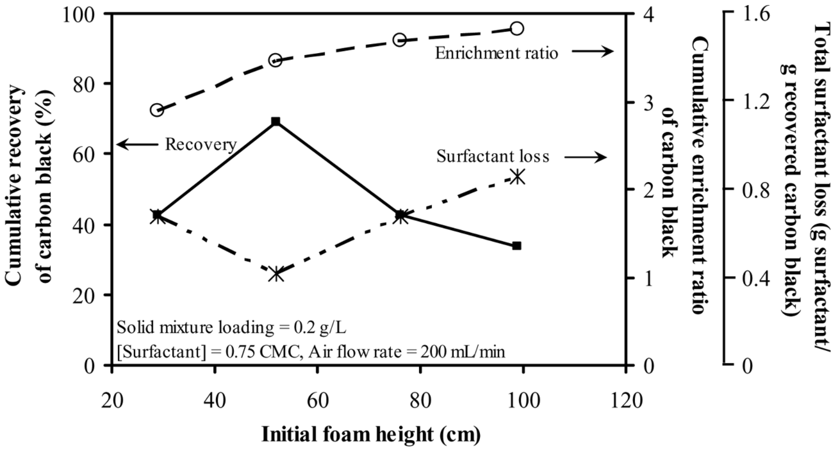

Figure 12. Effect of initial foam height on the recovery and enrichment ratio of carbon black and on surfactant loss.

Effects of NaCl Concentration

Normally, NaCl influences the performance of froth flotation because it affects the foam characteristics within a flotation column using anionic surfactants (19,20). Figure 13 shows that foamability and foam stability decrease when NaCl is initially added to the system. However, with increasing concentration of NaCl beyond 10 g/L, foamability increased;

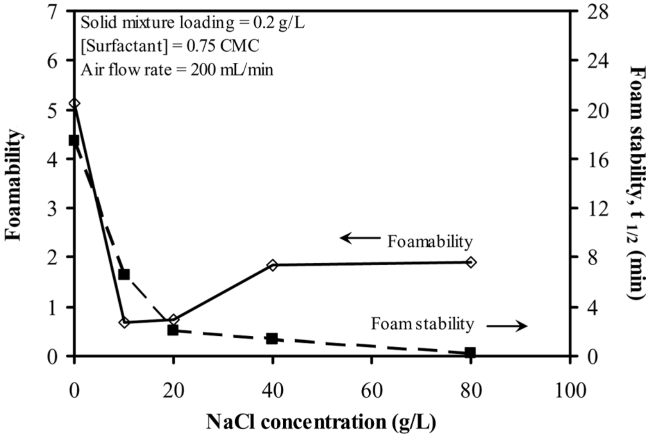

Figure 13. Effect of NaCl concentration on foamability and foam stability.

whereas foam stability further decreased. It was observed qualitatively that the foam bubbles became bigger, wetter, and more unstable when the NaCl content increased.

The recovery and enrichment ratio of carbon black, and the total surfactant loss, are depicted in Fig. 14 as a function of NaCl concentration. The recovery of carbon black mirrored the foamability; as it decreased then increased with increasing NaCl concentration. The carbon black enrichment ratio also mirrored the foamability, except at NaCl concentrations above 40 g/L where low foam stability caused a reduction in the enrichment ratio. The highest carbon black recovery and enrichment ratio, as well as the lowest total surfactant loss, corresponded to when there was no added NaCl; so adding an electrolyte does not aid the separation.

Air Bubble Size Distribution in Froth Flotation Column

In froth flotation, the separation performance also depends on the surface area flux of the air bubbles in the column. In the presence of a nonionic surfactant, like in this study, the surface of the air bubbles generated in the column is altered as a result of the surfactant adsorption at the air/water interface. A higher surface area flux means a greater possibility for carbon black to adhere to the air bubbles, which subsequently results in a higher carbon black recovery. The surface area flux of the air bubbles

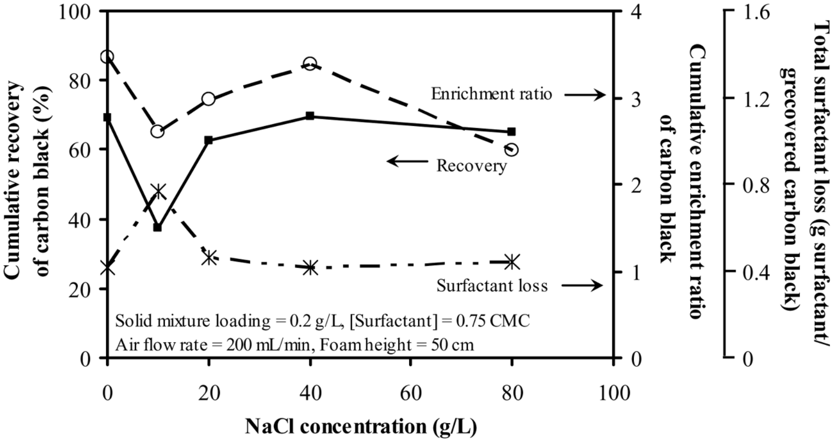

Figure 14. Effect of NaCl concentration on the recovery and enrichment ratio of carbon black and on surfactant loss.

is defined as the total surface area of air bubbles that rise across a given plane per second divided by the cross-sectional area of the flotation column. So, the bubble size distribution of the air bubbles during the flotation operation is required in order to calculate the surface area flux of the air bubbles.

The measurement of air bubble size distribution was done in the flotation column operated under the optimum conditions: an initial surfactant concentration of 0.75 times the CMC, a solid mixture loading of 0.2 g/L, an air flow rate of 200 mL/min, a foam height of 50 cm, and no added NaCl. The bubble size distributions at the beginning (0 min) and the end of operation (20 min) at the two positions (one-third and two-thirds of the initial liquid height) are shown in Figs. 15 and 16, respectively. The bubble size distributions as shown in both figures exhibit normal distribution curves with the air bubble sizes range between 400 and 4200 μm. In a comparison between the beginning and the end of operation (0 and 20 min), as shown in Figs. 15 and 16, for any given position, the air bubble diameter distribution at the beginning of the flotation is obviously narrower than that at the end of the operation. The liquid height has no significant effect on the bubble size distribution. In order to observe the effect of surfactant concentration, the change in the average air bubble diameter with time as compared to a pure water system is shown in Fig. 17. As expected, for the system with the surfactant, the average air bubble size increased with time. This is because the surfactant concentration decreases with time as the surfactant comes out with the foam. The effect of the position (the liquid height in the column) was found to be insignificant. The results confirm that the presence of the surfactant can reduce the coalescence rate of air bubbles in the column, leading to smaller bubble size than that of the pure water system. As shown in Figs. 17a and 17b, the presence of solid particles causes an increase in bubble size because of the surfactant loss by adsorption on the solid particles. The average bubble diameter from Fig. 17 is used to calculate the total surface area of air bubbles crossing the plane per second called as the surface area flux. Figure 18 shows the surface area flux of air bubbles as a function of time at the two positions for two cases of with and without solid mixture. It can be seen that the surface area flux of the system with no solid loaded decreased monotonically from 2.9 to 1.8 $m^2/m^2 \cdot min$ (at position 1) and the surface area flux in the system with 0.2 g/L solid mixture loading also decreased substantially from 2.7 to 1.7 $m^2/m^2 \cdot min$ (at position 1). The results suggest that the presence of the surfactant simply increases the surface area flux, which is responsible for solid separation of the froth flotation process. In addition, the presence of the solid particles decreased the surface area flux, because the air bubble size increased when the solid particles were added. For both cases of with and without the solid mixture for the surfactant containing system, the surface area flux of the air bubbles decreased with time and approached the value of the pure water system because of the depletion of the surfactant.

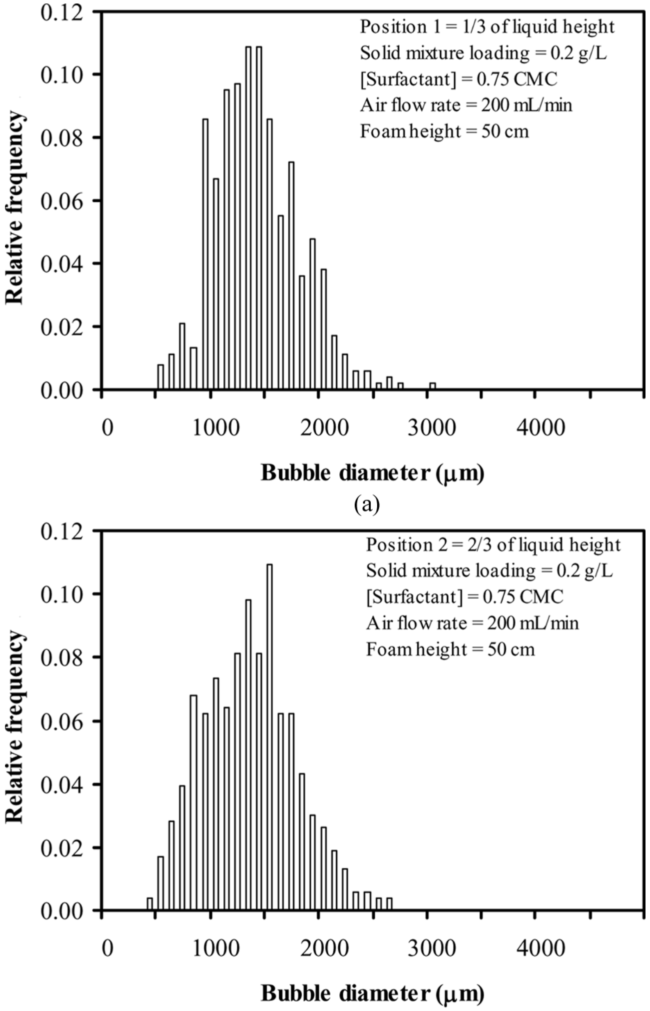

(a)

(b)

Figure 15. Relative frequency of air bubble diameters in the flotation column at 0 min operation time at (a) position 1 = 1/3 of liquid height from bottom and (b) position 2 = 2/3 of liquid height from bottom.

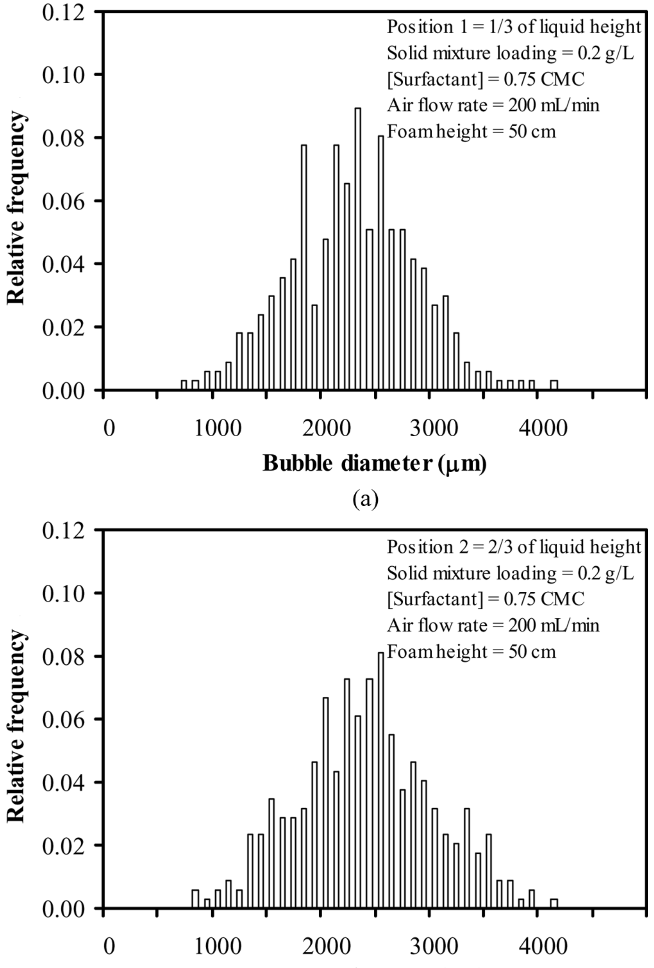

(a)

(b)

Figure 16. Relative frequency of air bubble diameters in the flotation column at 20 min operation time at (a) position 1 = 1/3 of liquid height from bottom and (b) position 2 = 2/3 of liquid height from bottom.

Moreover, the percentage either the carbon black or surfactant occupied on the air bubble surface was determined in order to clarify the selective separation mechanism of the hydrophobic carbon black particles in the froth flotation column. Based on an operation time of 20 min and the base conditions (61.6 μM surfactant concentration,

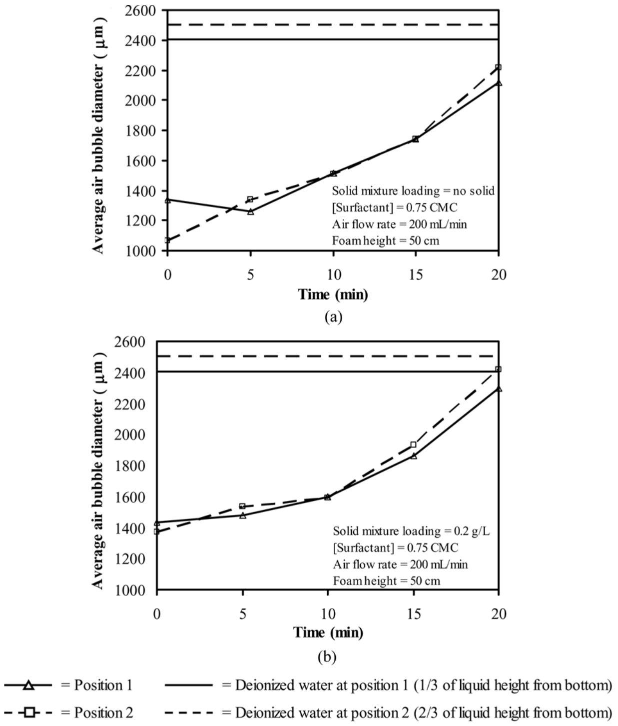

Figure 17. Average air bubble diameter as a function of operation time with (a) no addition of solid particles and (b) a solid mixture loading of 0.2 g/L.

0.2 g/L solid mixture loading, 200 mL/min air flow rate, and 50 cm foam height), the calculated air bubble surface coverage of carbon black and surfactant were 5.7, and 2.03% of the total area, respectively, suggesting that the separation efficiency of the carbon black from silica gel using froth flotation is not governed by the air bubble surface area flux. The low adsorption of both carbon black and surfactant on the air bubble surface is expected because of the short residence time of the air bubbles. Under the optimum conditions, the average residence time of the air bubbles in the column was found to be 3.2 s. Interestingly, the relatively high adsorption ratio of carbon black to the surfactant on the air bubble surface suggests the strong interaction between the carbon black particles and the nonionic surfactant, leading to the selective separation of carbon black from silica gel.

The effect of air bubble size distribution under different conditions will be presented in Part 2 in this series of papers.

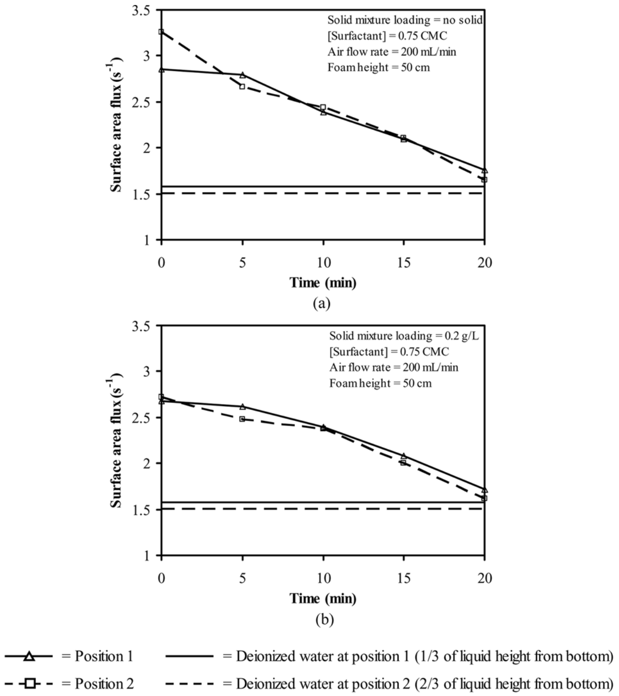

Figure 18. Surface area flux of air bubbles as a function of operation time with (a) no addition of solid particle and (b) a solid mixture loading of 0.2 g/L.

ACKNOWLEDGEMENTS

The Thailand Research Fund (TRF) is acknowledged for providing the Royal Golden Jubilee Ph.D. fellowships to Mr. Pisan Chungchamroenkit and Ms. Ummarawadee Yanatatsaneejit, as well as a research grant under TRF advanced research scholar to the corresponding author. The National Center of Excellence for Petroleum, Petrochemicals, and Advanced Materials, under The Ministry of Education, and The Research Unit: Applied Surfactants for Separation and Pollution Control, under The Ratchadapiseksompote Fund, Chulalongkorn University, are also acknowledged for providing research facilities and funding, respectively. Financial support for this research was also received from the industrial sponsors of the Institute for Applied Surfactant Research at the University of Oklahoma, including Akzo Nobel, Clorox, Conoco/ Phillips, Church and Dwight, Dow, Ecolab, Halliburton, Huntsman, Oxiteno, Procter & Gamble, Sasol, Shell, and Unilever.

REFERENCES

1. Fuerstenau, D.W.; Herrena-Urbina, R. (1989) Mineral separation by froth flotation. In *Surfactant-Based Separation Processes*; Scamehorn, J.F.; Harwell, J.H., eds.; Marcel Dekker, Inc.: New York, 259–320.
2. Yarar, B. (1997) Flotation. In *Encyclopedia of Separation Technology Vol. 2*; Ruthven, D.M., ed.; John Wiley & Sons: New York, 913–939.
3. Borchardt, J.K. (2000) Deinking of Papers Printed with Water-Based Inks: An Overview. In *Surfactant-Based Separations: Science and Technology*; Scamehorn, J.F.; Harwell, J.H., eds.; American Chemical Society: Washington DC., 384–419.
4. Choi, S.J.; Choi, Y.H. (1996) Removal of direct red from aqueous solution by foam separation techniques of ion and adsorbing colloid flotation. *Sep. Sci. Technol.*, *31*: 2105–2116.
5. Zouboulis, A.I.; Lazaridis, N.K.; Zamboulis, D. (1994) Powdered activated carbon separation from water by foam flotation. *Sep. Sci. Technol.*, *29*: 385–400.
6. Iijima, S.; Ichihashi, T. (1993) Single-shell carbon nanotubes of 1-nm diameter. *Nature*, *363*: 603–605.
7. Bethune, D.S.; Kiang, C.H.; de Vries, M.S.; Gorman, G.; Savoy, R.; Vazquez, J.; Beyers, R. (1993) Cobalt-catalysed growth of carbon nanotubes with single-atomic-layer walls. *Nature*, *363*: 605–607.
8. Yakobson, B.I.; Smalley, R.E. (1997) Fullerene Nanotubes: $C_{1,000,000}$ and beyond. *Am. Sci.*, *85*: 324–337.
9. Ajayan, P.M.; Zhou, O.Z. (2001) Applications of carbon nanotubes. *Top. Appl. Phys.*, *80*: 391–425.
10. Kitiyanan, B.; Alvarez, W.E.; Harwell, J.H.; Resasco, D.E. (2000) Controlled production of single-wall carbon nanotubes by catalytic decomposition of CO on bimetallic Co–Mo catalysts. *Chem. Phys. Lett.*, *317*: 497–503.
11. Henrard, L.; Hernandez, E.; Bernier, P.; Rubio, A. (1999) Van der Waals interaction in nanotube bundles: consequences on vibrational modes. *Phys. Rev. B*, *60*: R8521–R8524.
12. Park, J.; Regalbuto, J.R. (1995) A simple, accurate determination of oxide PZC and the strong buffering effect of oxide surfaces at incipient wetness. *J. Colloid Interface Sci.*, *175*: 239–252.
13. Scamehorn, J.F.; Sabatini, D.A.; Harwell, J.H. (2004) Surfactants, Part I: Fundamentals. In *Encyclopedia of Supramolecular Chemistry*; Atwood, J.; Stead, J., eds.; Marcel Dekker, Inc.: New York, 1458–1469.
14. Rosen, M.J. (1989) *Surfactant and Interfacial Phenomena,* 2nd Ed.; John Wiley & Sons: New York, 276–303.
15. Scamehorn, J.F.; Sabatini, D.A.; Harwell, J.H. (2004) Surfactants, Part II: Applications. In *Encyclopedia of Supramolecular Chemistry*; Atwood, J.; Stead, J., eds.; Marcel Dekker, Inc.: New York, 1470–1477.
16. Zhao, Y.; Deng, Y.; Zhu, J.Y. (2004) Roles of surfactants in flotation deinking. *Prog. Pap. Recycl.*, *14*: 41–45.
17. Pondstabodee, S.; Scamehorn, J.F.; Chavadej, S.; Harwell, J.F. (1998) Cleanup of oily wastewater by froth flotation: Effect of microemulsion formation. *Sep. Sci. Technol.*, *33*: 591–609.

18. Chavadej, S.; Phoochinda, W.; Yanatatsaneejit, U.; Scamehorn, J.F. (2004) Clean-up of oily wastewater by froth flotation: effect of microemulsion formation III: Use of anionic/nonionic surfactant mixtures and effect of relative volumes of dissimilar phases. *Sep. Sci. Technol.*, *29*: 3021–3036.
19. Yanatatsaneejit, U.; Witthayapanyanon, A.; Ransunvigit, P.; Acosta, E.J.; Sabatini, D.A.; Scamehorn, J.F.; Chavadej, S. (2005) Ethylbenzene removal by froth flotation under conditions of middle-phase microemulsion formation I: Interfacial tension, foamability, and foam stability. *Sep. Sci. Technol.*, *40*: 1537–1553.
20. Yanatatsaneejit, U.; Rangsunvigit, P.; Scamehorn, J.F.; Chavadej, S. (2008) Diesel oil removal by froth flotation under low interfacial tension conditions I: Foam characteristics, and equilibration time. *Sep. Sci. Technol.*, *43*: 1520–1534.
21. Kralchevsky, P.A.; Nagayama, K. (2001) *Particles at Fluid Interfaces and Membranes*; Elsevier: Amsterdam, 591–633.
22. Koutlemani, M.M.; Mavros, P.; Zouboulis, A.I.; Matis, K.A. (1994) Recovery of Co^{2+} ions from aqueous solutions by froth flotation. *Sep. Sci. Technol.*, *29*: 867–886.